



ELSEVIER

Contents lists available at ScienceDirect

Comptes Rendus Chimie

www.sciencedirect.com



Full paper/Mémoire

Ultrasonic-bath-assisted preparation of mononuclear copper(I) thiosemicarbazone complex particles: Crystal structure, characterization and antimicrobial activity



Aliakbar Dehno Khalaji ^{a, b, *}, Ensieh Shahsavani ^c, Nourollah Feizi ^c,
Monika Kučeráková ^d, Michal Dušek ^d, Rauof Mazandarani ^e, Ahmad Amiri ^f

^a Department of Chemistry, Faculty of Science, Golestan University, Gorgan, Iran

^b Cubane Chemistry of Hircane Co. Gorgan, Iran

^c Department of Chemistry, Payame Noor University, PO Box 19395-3697, Tehran, Iran

^d Institute of Physic ASCR, v. v. i., Na Slovance 2, 182 21, Prague, Czech Republic

^e Department of Biochemistry, Faculty of Science, Golestan University, Gorgan, Iran

^f Department of Chemistry, College of Science, University of Tehran, Tehran 14155-6455, Iran

ARTICLE INFO

Article history:

Received 17 February 2016

Accepted 10 May 2016

Available online 28 June 2016

Keywords:

Thiosemicarbazone

Copper(I) complex

Spectroscopy

X-ray crystallography

ABSTRACT

Particles of the copper(I) thiosemicarbazone complex $[\text{Cu}(\text{Brcatsc})(\text{PPh}_3)_2\text{Cl}]\cdot\text{CH}_3\text{CN}$ (**1**), Brcatsc = 2-bromo-3-phenylpropenalthiosemicarbazone, were synthesized by an ultrasonic-bath-assisted method and characterized by elemental analyses, NMR (^1H , ^{13}C , and ^{31}P) and FT-IR spectroscopies, X-ray powder diffraction (XRD) and scanning electron microscopy (SEM). The thermal stability of **1** was studied by thermal gravimetry analysis and its structure was determined by single crystal X-ray diffraction. The compound **1** is a mononuclear complex with the copper(I) ion coordinated in a distorted tetrahedral geometry by one S atom of Brcatsc, two P atoms of two PPh_3 , and one Cl atom. The complex involves the Brcatsc thiosemicarbazone ligand in an S monodentate bonding mode. The antibacterial activity of the ligand and its copper(I) complex was studied against two gram-positive (*Staphylococcus aureus* and *Enterococcus faecalis*) and two gram-negative (*Escherichia coli* and *Pseudomonas aeruginosa*) bacteria.

© 2016 Académie des sciences. Published by Elsevier Masson SAS. All rights reserved.

1. Introduction

Thiosemicarbazone molecules with nitrogen and sulfur donor atoms are important ligands in coordination chemistry [1,2]. Their complexes with a transition metal have interesting biological and chemical properties [1,2], variable bonding features, and considerable structural diversity [3–11]. The biological properties of thiosemicarbazone

complexes are often related to the coordination pathway towards the transition metal ion [2–5]. Thiosemicarbazones bind to the transition metal center in a neutral or anionic form [1–11]. Variable bonding and structural diversity of metal complexes with thiosemicarbazone derivatives were reviewed in 2009 by Lobana and his co-workers [12]. Copper(I) forms both charged and neutral complexes with thiosemicarbazone ligands [13–23]. Moreover, it was found that the substituents at the carbon atom of the imine group ($\text{C}=\text{N}$) affect the bonding to the copper(I) halides, determining the formation of mono-, di- and poly-nuclear complexes. Often, these complexes crystallize in the presence of PPh_3 as a co-ligand.

* Corresponding author. Department of Chemistry, Faculty of Science, Golestan University, Gorgan, Iran.

E-mail address: alidkhalaji@yahoo.com (A. Dehno Khalaji).

Following our previous work on thiosemicarbazone complexes [24–26], here we report a simple ultrasonic-bath-assisted preparation of (nano)particles of a mononuclear copper(I) complex $[\text{Cu}(\text{Brcatsc})(\text{PPh}_3)_2\text{Cl}]\cdot\text{CH}_3\text{CN}$ (**1**) (Scheme 1), which is synthesized by the reaction of CuCl , Brcatsc and PPh_3 (molar ration 1:1:2).

2. Experimental

2.1. Reagents and physical measurements

All reagents and solvents for synthesis and analysis were obtained from Merck and used as received. The thiosemicarbazone ligand Brcatsc was prepared in high yield following the literature [27]. The FT-IR spectrum was recorded in the range $400\text{--}4000\text{ cm}^{-1}$ on a PerkinElmer FT-IR spectrophotometer using KBr pellets. Elemental analyses were performed on a Heraeus CHN-O-Rapid analyzer and the results agreed with the calculated values. ^1H , ^{13}C and ^{31}P NMR spectra were recorded on a BRUKER DRX-400 AVANCE spectrometer at 300 MHz for the Schiff base ligand. All chemical shifts are reported in δ units downfield from tetramethylsilane (TMS). The thermogravimetric analysis (TG) was performed in the temperature range $30\text{--}750\text{ }^\circ\text{C}$ on a PerkinElmer TG/DTA lab system 1 (technology by SII). The samples were held in a nitrogen atmosphere and a heating rate of $20\text{ }^\circ\text{C}/\text{min}$ was set. X-ray powder diffraction was performed on a Philips X'pert diffractometer using $\text{Cu K}\alpha$ radiation. The SEM images were obtained using a Philips XL 30 scanning electron microscope. The samples were made conductive by a thin gold coating. UV–vis spectra were recorded on a PerkinElmer Lambda 25 spectrometer.

2.2. Antibacterial activity

The antibacterial performance of Brcatsc and its copper(I) complex **1** was investigated against two gram-positive (*Staphylococcus aureus* ATCC-25923 and *Enterococcus faecalis* ATCC-29212) and two gram-negative (*Escherichia coli* ATCC 25922 and *Pseudomonas aeruginosa* ATCC-27853) bacteria. The tests were performed using a methodology described in the guidelines of the Comité de l'Antibiogramme de la Société Française de Microbiologie (CA-SFM, www.sfm.asso.fr) [28]. A solution of Brcatsc and **1** was prepared at $20\text{ mg}/\text{mL}$ in DMSO under sterile conditions. After dilution, 10 Petri plates were prepared with concentrations from 10 to $100\text{ }\mu\text{g}/\text{mL}$ (increasing by $10\text{ }\mu\text{g}/\text{mL}$). The different Petri plates were inoculated by $\approx 2 \times 10^4$

bacteria suspended in sterile distilled water. After 24 h incubation at $37\text{ }^\circ\text{C}$, the minimum inhibitory concentration (MICs, $\mu\text{g}/\text{mL}$) was determined.

2.3. X-ray structure determination

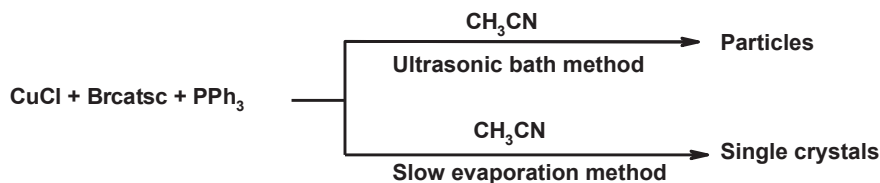
A single crystal of dimensions $0.11 \times 0.08 \times 0.07\text{ mm}^3$ was chosen for the X-ray diffraction study. Crystallographic measurements were performed at 120 K with a four-circle CCD diffractometer Gemini (Oxford diffraction, Ltd.), equipped with mirror-collimated $\text{Cu K}\alpha$ radiation ($\lambda = 1.54184\text{ \AA}$). Although the quality of the single crystals was not the best (as indicated, e.g., by the R_{int} factor in Table 1), the crystal structure could be easily solved by the charge flipping program SUPERFLIP [29]. The refinement was carried out by the Jana2006 program package [30] employing a full-matrix least-squares technique on F^2 . The molecular structure plots were prepared by Diamond 4.0 [31]. The hydrogen atoms were mostly discernible in difference Fourier maps and could be refined to a reasonable geometry. According to common practice, the hydrogen atoms attached to carbons were kept in ideal positions during the refinement with a C–H distance of 0.96 \AA and their isotropic atomic displacement parameters were set to $1.2U_{\text{eq}}$ of their parent atoms. Crystallographic data, details of the data collection, structure solution, and refinements are listed in Table 1.

This complex has disordered acetonitrile molecules. Two positions of this linear molecule, with refined occupancy of 0.775(12) and 0.225(12), are oriented in such a way that they almost coincide on one side but are considerably deviated on the opposite side. The decision whether the overlapped part combines two close nitrogen atoms or one nitrogen and one CH_3 group was further complicated by a smeared difference in the electron density in this area without clear indication of the hydrogen atoms. Refinement of two structure models indicated that the two disordered acetonitrile molecules have probably opposite orientations, combining N and CH_3 , because this model yielded a geometry closer to linear and better interatomic distances.

2.4. Preparation of **1**

2.4.1. Slow evaporation

Solid PPh_3 (0.052 g, 0.2 mmol) was added to CuCl (0.009 g, 0.1 mmol) suspended in acetonitrile (10 mL), and the mixture was stirred for 0.5 h. To this mixture, the Brcatsc ligand in the solid state was added (0.028,



Scheme 1. Materials produced and synthetic methods.

Table 1
Crystallographic data and structural refinement details of **1**.

Empirical Formula	C ₄₈ H ₄₁ Br ₁ C ₁₁ Cu ₁ N ₄ P ₂ S ₁
Formula weight	946.8
Crystal system, space group	Triclinic, <i>P</i> $\bar{1}$
<i>a</i> , Å	10.5899(4)
<i>b</i> , Å	13.4301(6)
<i>c</i> , Å	17.0554(8)
α , deg	68.874(4)
β , deg	80.139(3)
γ , deg	88.483(3)
<i>V</i> , Å ³	2227.58(18)
<i>Z</i>	4
μ , mm ⁻¹	5.52
Measured/independent reflections	12,950/7586
<i>R</i> _{int}	0.084
Reflections with <i>I</i> > 3 σ (<i>I</i>)	7822
Parameters	1045
<i>S</i>	1.52
<i>R</i> (<i>F</i> ² > 3 σ (<i>F</i> ²))	0.043
<i>wR</i> (<i>F</i> ²)	0.053

0.1 mmol), and the content was stirred until a clear solution was obtained. The solution was allowed to evaporate slowly at room temperature for several days. The white polygonal crystals were filtered, washed twice with acetonitrile, and dried at room temperature (0.65 g, 75.6%). *Anal. calcd.* for C₄₈H₄₁BrClCuN₄P₂S₁: C, 60.89; H, 4.33; N, 5.92; S, 3.38%. *Found:* C, 60.38; H, 4.8; N, 5.77; S, 4.08%. FT-IR data (KBr, cm⁻¹): ν (N–H) 3150, ν (–NH₂ group), 3264–3427, ν (C–H aromatic) 3049, ν (C–H imine) 2802, ν (–C=N imine) 1591, ν (C=C aromatic) 1537, { ν (C–N) + ν (C–C) + ν (P–C_{ph}) } 1028, 1097, 1175, ν (C=S) 854, ν (Cu–S) 510. ¹H NMR (DMSO-*d*₆, δ ppm): 11.9 (s, 1H, –NH), 8.6 (s, 1H, C^bH), 7.9 (d, 1H, C^bH), 7.6 (d, 2H, –NH₂), 7.2–7.4 (m, 31H, PPh₃ + C^dH), 7.0–7.1 (d, 2H, C^{f,j}H), 6.8–6.9 (dd, 2H, C^{g,i}H). ¹³C NMR (DMSO-*d*₆, δ ppm): 176.1 (C^a=S), 146.6 (C^b=N), 125.0–140.1 (C^{c–j} + PPh₃). ³¹P NMR (DMSO-*d*₆, δ , ppm): –5.5.

2.4.2. Ultrasonic bath

In order to prepare particles of **1**, 10 mL of CuCl (0.1 mmol) in acetonitrile was placed in an ultrasonic bath, with a power output of 40 KHz. Into this solution, a 10 mL solution of Brcatsc (0.1 mmol) and PPh₃ (0.2 mmol) was added dropwise. The obtained precipitate was filtered off, washed with acetonitrile and then dried in air (0.78 g, 90.7%). FT-IR data (KBr, cm⁻¹): ν (–NH₂ group) 3418, 3266, ν (–NH–) 3137, ν (C–H aromatic) 3050, ν (–C=N imine) 1592, ν (C–C) 1537–1479, ν (C–N) 1096, ν (C=S) 932, 853.

3. Results and discussion

3.1. Synthesis and spectroscopic characterization

The reaction of Brcatsc with an acetonitrile solution of copper(I) chloride (CuCl) (1:1 molar ratio), followed by the addition of triphenyl phosphine (PPh₃), yielded bright yellow crystals of the mononuclear copper(I) thiosemicarbazone complex of empirical formula [Cu(Brcatsc)(PPh₃)₂Cl]·CH₃CN (**1**) (Fig. 1). The elemental analysis revealed that the ratio of Brcatsc, PPh₃ and CuCl was 1:2:1. To our knowledge this is the first copper(I)

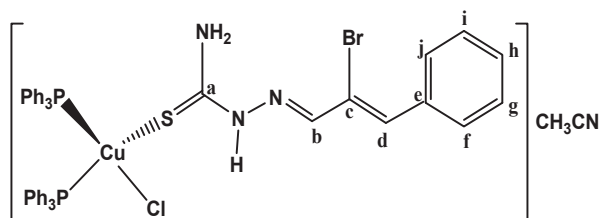


Fig. 1. The chemical structure of **1**.

thiosemicarbazone complex containing bromocinnamaldehyde.

The FT-IR spectrum of the complex (Fig. 2) is similar to the one of the free ligand [27] along with some distinct changes in the position of the bands. The presence of three ν (N–H) bands at 3150 cm⁻¹ (due to –N–NH–C) and 3264–3427 cm⁻¹ (due to –NH₂) indicates the coordination of a neutral ligand in the complex. In addition, the characteristic bands of ν (C=S) and ν (C=N) vibrational modes as seen at 854 and 1591 cm⁻¹, respectively, indicate the presence of the ligand. The shifting of the ν (C=S) band to a higher energy in the complex compared to the free ligand (859 cm⁻¹) confirms that the Brcatsc ligand is coordinated to copper(I) by the S-donor atom. Further, ν (C–H aromatic) and { ν (P–C_{ph}) + ν (C–C) + ν (C–N) } bands are present at 3049 cm⁻¹ and in the range 1028–1175 cm⁻¹, respectively [16,18,25]. As shown in Fig. 2, the FT-IR spectra of the complex **1** prepared by the two different methods are similar.

¹H, ¹³C and ³¹P NMR spectra of **1** were recorded using DMSO-*d*₆ as the solvent and are shown in Fig. 3. The ¹H NMR spectrum of **1** (Fig. 3a) exhibited the N–NH–C=S

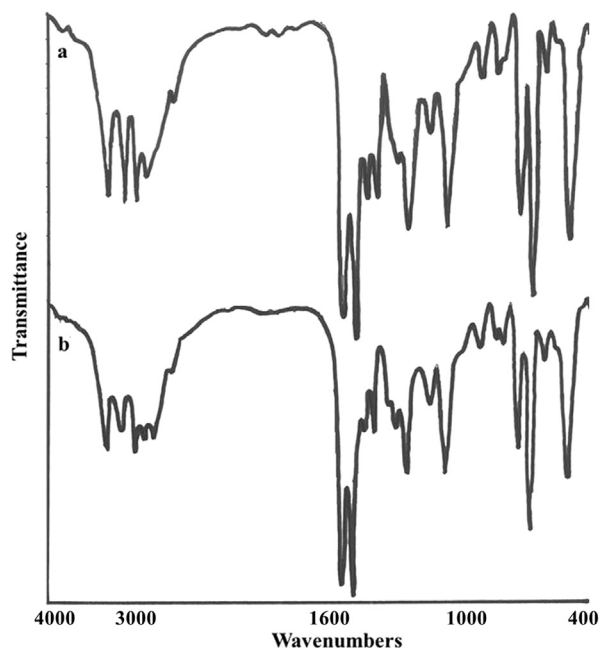


Fig. 2. FT-IR spectrum of **1** prepared by two different routes: a) slow evaporation and b) ultrasonic bath.

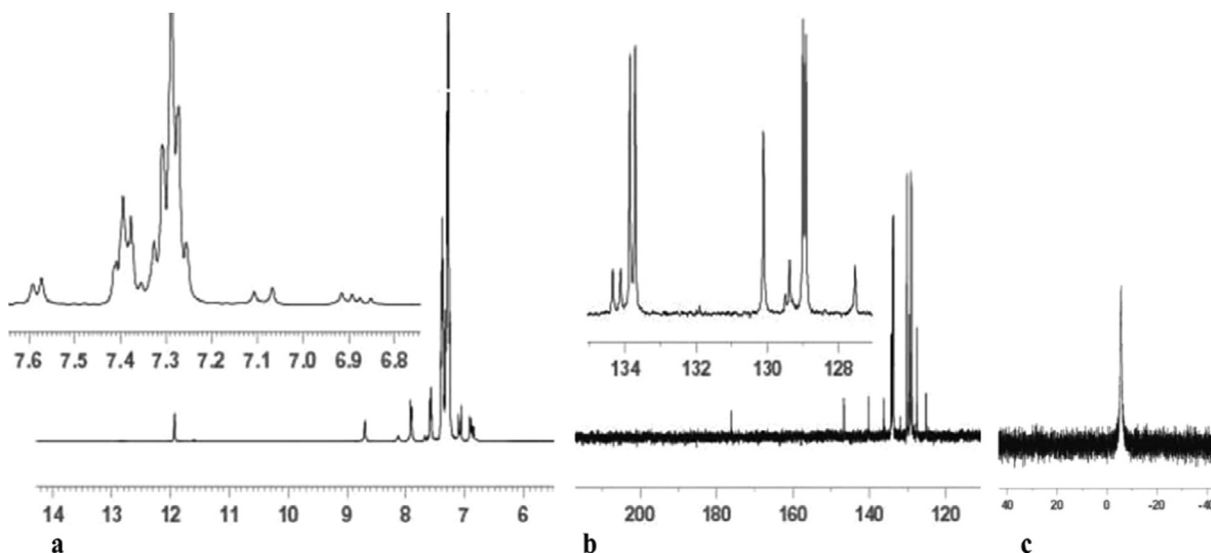


Fig. 3. NMR spectra of **1**: a) ^1H , b) ^{13}C , and c) ^{31}P .

singlet signal at about 11.5 ppm, indicating coordination of the ligand to the copper(I) ion in its neutral form, probably via the S-donor atom [25,26]. A singlet signal ≈ 8.5 ppm also reveals the presence of the iminic hydrogen ($-\text{CH}=\text{N}-$). The aromatic protons of Brcatsc in **1** appear as three signals at 7.0–7.1 (d, 2H, $\text{C}^{\text{f}}\text{H}$, $J = 16$ Hz), 6.8–6.9 (dd, 2H, $\text{C}^{\text{g}}\text{H}$, $J = 16$ Hz) and 7.9 ppm (d, 1H, $\text{C}^{\text{h}}\text{H}$, $J = 8$ Hz). The ethylenic proton ($\text{C}^{\text{d}}\text{H}$) and aromatic protons of PPh_3 are present in the range 7.26–7.41 ppm (m, 31H, $\text{PPh}_3 + \text{C}^{\text{d}}\text{H}$). The amine protons ($-\text{NH}_2$) of Brcatsc appeared as doublet signals at about 7.90 ppm. The aromatic protons of PPh_3 appear between 7.26 and 7.41 ppm [25,26].

The ^{13}C NMR spectrum (Fig. 3b) also shows signals for the carbon atoms of $\text{C}^{\text{a}}=\text{S}$ and $\text{C}^{\text{b}}=\text{N}$ groups at 175 and 145 ppm, respectively. Other carbons (aromatic and ethylenic) can be seen as signals in the interval 120–145 ppm. The ^{31}P NMR spectrum of **1** (Fig. 3c) shows only a singlet peak at 5.55 ppm for the two P atoms, which confirms their equivalent chemical environment. Moreover, it points that the geometry around the copper(I) ion is tetrahedral and not square-planar, which is in agreement with the bonding angles involving the copper(I) ion ranging from 102.48 to 125.11°.

3.2. Crystal structure of **1**

Complex **1** crystallizes in the triclinic crystal system (space group $\text{P}\bar{1}$). The triclinic unit cell contains two molecules of the complex. The molecular structure of **1** is depicted in Fig. 4. Selected bond distances and angles are presented in Table 2. In **1**, the copper(I) ion is bonded to one chlorine atom, one sulfur atom (of the Brcatsc ligand), and two phosphorous atoms from two PPh_3 groups, forming a distorted tetrahedral geometry around the Cu(I) center. The bond distances Cu1–S1 (2.3650(16) Å), Cu1–Cl1 (2.3911(15) Å), Cu1–P1 (2.2738(18) Å) and Cu1–P2 (2.2586(18) Å) are similar to those reported for other mononuclear copper(I) thiosemicarbazone complexes [15–17,24]. Bond distances and different bond angles are

given in Table 2 and confirm the distorted tetrahedral geometry around the copper(I) center in **1** [15–17,24].

As mentioned above, the bond angles around Cu vary from 102.48 to 125.11°, indicating a distorted tetrahedral geometry. The maximum deviation from 109.5° was found for the P1–Cu1–P2 angle (125.11°) and can be explained by the presence of six aromatic rings in the two PPh_3 [15–17]. The sulfur atom S1 and the hydrazinic nitrogen N3 are in the *E* position with respect to the C11–N2 bond. The stability of this configuration in the thiosemicarbazone ligand is due to the presence of an intra-molecular hydrogen bond ($\text{N2}-\text{H1}\cdots\text{Cl1}$). The coordination of the Brcatsc ligand to copper(I) via the sulfur atom causes a decrease of the C=S bond distance in the complex (1.689(7) Å) compared to the free ligand (1.702(5) Å) [26].

3.3. TGA of **1**

To examine the thermal stability of **1**, thermogravimetry (TG) was carried out between 30 and 750 °C under a nitrogen flow (Fig. 5). The compound **1** was found to be stable up to about 250 °C. Decomposition of **1** occurs between 250 and 700 °C with a total mass loss of 85%.

3.4. XRD and SEM of **1**

Fig. 6 shows the XRD pattern of **1** prepared in an ultrasonic bath. The relatively sharp peaks indicates that the particles are of micrometric size and that the Scherrer formula can be used for calculation of the crystallites size forming the particles. Fig. 7 shows the scanning electron microscopy of **1** at two different scales. The SEM images show uniform morphology of the aggregated particles.

3.5. Antibacterial activity

The antibacterial activity of Brcatsc and its copper(I) complex prepared by the two methods discussed above was

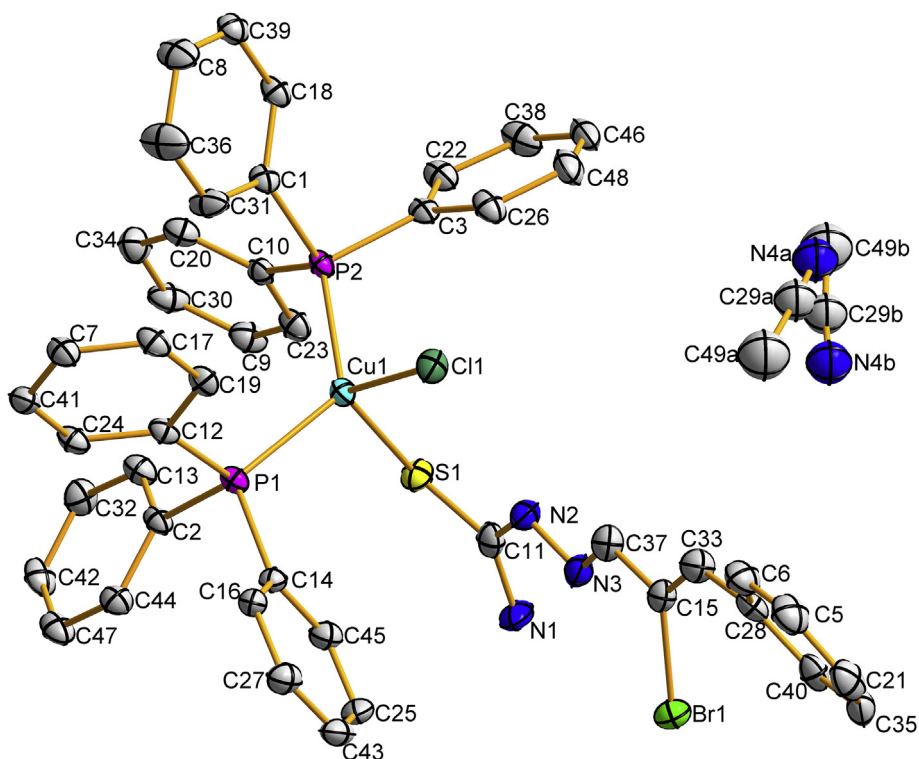


Fig. 4. Molecular structure of **1** with atomic displacement ellipsoids shown at a 40% probability level. H atoms are omitted for clarity. The disorder of the acetonitrile is explained in Section 2.4.

Table 2

Selected bond distances (Å) and angles (°) of **1**.

Bond lengths in Å		Bond angles in degrees	
Cu1–Cl1	2.3911(15)	Cl1–Cu1–P1	103.70(5)
Cu1–S1	2.3650(16)	Cl1–Cu1–P2	108.02(5)
Cl1–N2	3.129(6)	P1–Cu1–P2	125.11(7)
S1–C11	1.689(7)	Cl1–Cu1–S1	111.72(6)
N1–C11	1.324(9)	P1–Cu1–S1	105.75(5)
N2–C11	1.364(7)	S1–Cu1–P2	102.48(6)
Cu1–P1	2.2738(13)	Cl1–N2–C11	118.2(4)
Cu1–P2	2.2586(18)	N2–N3–C37	115.4(6)
N2–N3	1.362(9)	Cl1–N2–N3	119.1(3)
N3–C37	1.279(7)	N3–N2–C11	119.3(5)
		Cu1–Cl1–N2	74.39(10)

studied against gram-positive (*E. faecalis* and *S. aureus*) and gram-negative (*E. coli* and *P. aeruginosa*) bacteria. The results show that the Bratsc has no antibacterial activity against

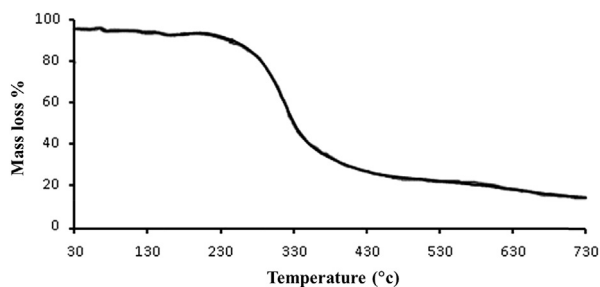


Fig. 5. Thermogram of **1**.

any of the tested bacteria even in concentrations as high as 500 µg/mL, while the complex is active against the gram-positive bacterial strains. The tested Petri plates are shown in Fig. 8. The MIC value (Table 3) of the complex against both *E. faecalis* and *S. aureus* is 70 µg/mL. The increased antibacterial activity of **1** compared to that of Bratsc is due to the difference in the structures, which influences the attack on the cell walls of the bacteria [32,33]. In addition, the antibacterial activity of the complex prepared by two different methods was found to be similar.

4. Conclusion

A new copper(I) complex containing thiosemicarbazone was synthesized and characterized. Single-crystal structure

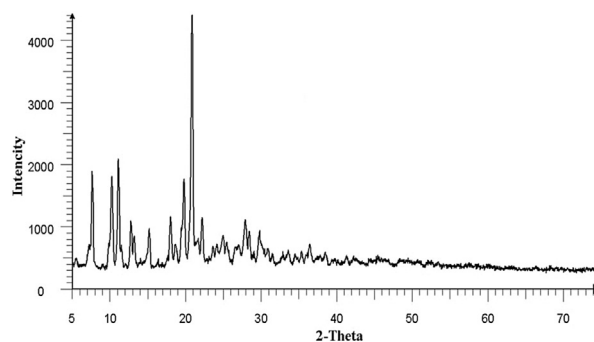


Fig. 6. XRD pattern of **1** prepared in an ultrasonic bath.

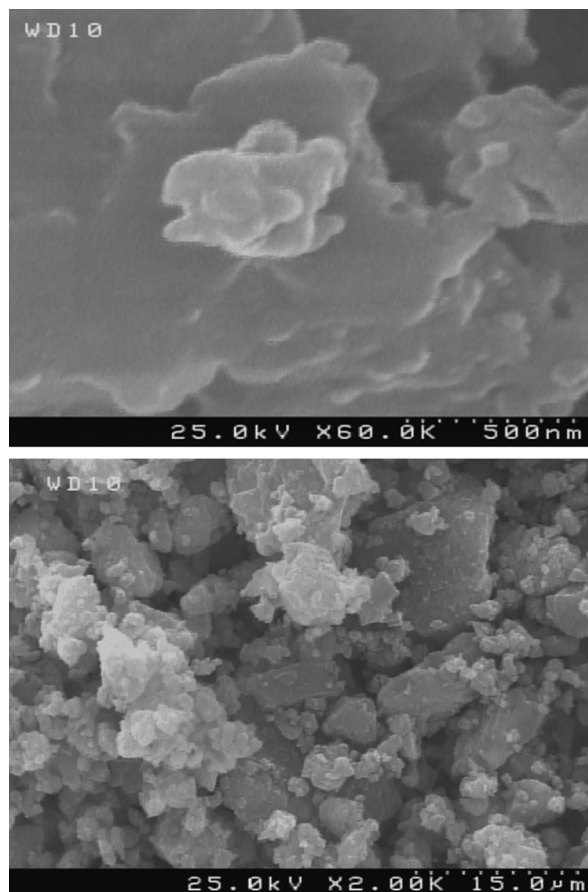


Fig. 7. SEM images of **1** prepared in an ultrasonic bath.

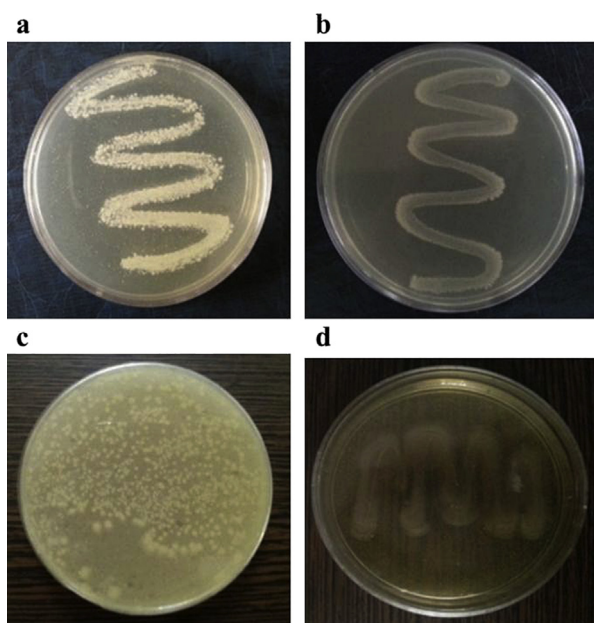


Fig. 8. The antibacterial screening of **1** with 60 $\mu\text{g/mL}$ concentration against a) *S. aureus*, b) *E. faecalis*, c) *E. coli* and d) *P. aeruginosa*.

Table 3

The MIC value ($\mu\text{g/mL}$) of the ligand and the complex.

	MIC of the complex	MIC of the Bratcsc ligand
<i>E. faecalis</i> (ATCC29212)	70	>500
<i>S. aureus</i> (ATCC25923)	70	>500
<i>E. coli</i> (ATCC25922)	>500	>500
<i>P. aeruginosa</i> (ATCC2753)	>500	>500

determination showed that the copper(I) ion is coordinated with one S atom (of Bratcsc), one Cl and two P atoms in a distorted tetrahedral geometry. The spectroscopy data confirmed that the Bratcsc and PPh_3 coordinate the copper(I) ion. An antibacterial screening indicated that the copper(I) complex exhibits considerably higher antibacterial activity than the free ligand towards gram-positive bacteria.

Acknowledgments

We are grateful to the Payame Noor University and Golestan University for financial support of this work. The crystallography was supported by the project 15-12653S of the Czech Science Foundation using instruments of the ASTRA lab established within the Operation program Prague Competitiveness—project CZ.2.16/3.1.00/24510.

Supplementary data

Crystallographic data (excluding structure factors) for the structure reported in this paper have been deposited with the Cambridge Crystallographic Center, CCDC No. 1042028. Copies of the data can be obtained free of charge on deposit@ccdc.cam.ac.uk or <http://www.ccdc.cam.ac.uk>.

References

- [1] D.G. Calatayud, E. Lopez-Torres, M. Antonia Mendiola, *Polyhedron* 101 (2015) 133–138.
- [2] P.P. Netalkar, S.P. Netalkar, V.K. Revankar, *Polyhedron* 100 (2015) 215–222.
- [3] S. Chandra, Vandana, *Spectrochim. Acta A* 129 (2014) 333–338.
- [4] T.P. Stanojkovic, D. Kovala-Demertzi, A. Primikyri, I. Garcia-Santos, A. Castineiras, Z. Juranic, M.A. Demertzis, *J. Inorg. Biochem.* 104 (2010) 467–476.
- [5] D. Kovala-Demertzi, A. Alexandratos, A. Papageorgiou, P.N. Yadav, P. Dalezis, M.A. Demertzis, *Polyhedron* 27 (2008) 2731–2738.
- [6] T.S. Lobana, R. Sharma, R.J. Butcher, *Polyhedron* 28 (2009) 1103–1110.
- [7] T.S. Lobana, S. Khanna, A. Castineiras, *Inorg. Chem. Commun.* 10 (2007) 1307–1310.
- [8] T.S. Lobana, S. Khanna, R. Sharma, G. Hundal, R. Sultana, M. Chaudhary, R.J. Butcher, A. Castineiras, *Cryst. Growth Des.* 8 (2008) 1203–1212.
- [9] A. Castineiras, N. Fernandez-Hermida, I. Garcia-Santos, J.L. Perez-Lustres, I. Rodriguez-Gonzalez, *Dalton Trans.* 41 (2012) 3787–3793.
- [10] A. Castineiras, R. Pedrido, *Inorg. Chem.* 47 (2008) 5534–5536.
- [11] A. Castineiras, R. Pedrido, *Inorg. Chem.* 48 (2009) 4847–4855.
- [12] T.S. Lobana, R. Sharma, G. Bawa, S. Khanna, *Coord. Chem. Rev.* 253 (2009) 977–1055.
- [13] T.S. Lobana, S. Khanna, R.J. Butcher, *Dalton Trans.* 41 (2012) 4845–4851.
- [14] T.S. Lobana, P. Kumari, R. Sharma, A. Castineiras, R.J. Butcher, T. Akitsu, Y. Aritake, *Dalton Trans.* 40 (2011) 3219–3228.
- [15] T.S. Lobana, P. Kumari, R.J. Butcher, *Inorg. Chem. Commun.* 11 (2008) 11–14.

- [16] T.S. Lobana, S. Khanna, R.J. Butcher, A.D. Hunter, M. Zeller, *Inorg. Chem.* 46 (2007) 5826–5828.
- [17] T.S. Lobana, R. Sharma, A. Castineiras, R.J. Butcher, *Z. Anorg. Allg. Chem.* 636 (2010) 2698–2703.
- [18] T.S. Lobana, R. Sharma, G. Hundal, A. Castineiras, R.J. Butcher, *Polyhedron* 47 (2012) 134–142.
- [19] T.S. Lobana, Rekha, R.J. Butcher, A. Castineiras, E. Bermejo, P.V. Bharatam, *Inorg. Chem.* 45 (2006) 1535–1542.
- [20] T.S. Lobana, S. Khanna, G. Hundal, R.J. Butcher, A. Castineiras, *Polyhedron* 28 (2009) 3899–3906.
- [21] T.S. Lobana, S. Khanna, A. Castineiras, G. Hundal, *Z. Anorg. Allg. Chem.* 636 (2010) 454–456.
- [22] T.S. Lobana, R. Sharma, *Z. Anorg. Allg. Chem.* 635 (2009) 2150–2152.
- [23] T.S. Lobana, S. Khanna, R.J. Butcher, *Z. Anorg. Allg. Chem.* 633 (2007) 1820–1826.
- [24] A.D. Khalaji, G. Grivani, M. Rezaei, K. Fejfarova, M. Dusek, *Phos. Sulf. Sil* 188 (2013) 1119–1126.
- [25] E. Shahsavani, A.D. Khalaji, N. Feizi, M. Kucerakova, M. Dusek, *Inorg. Chim. Acta* 429 (2015) 61–66.
- [26] E. Shahsavani, A.D. Khalaji, N. Feizi, M. Kucerakova, M. Dusek, *Superlattices Microstruct.* 82 (2015) 18–25.
- [27] N.M. Samus, Y.M. Chumakov, V.I. Tsapkov, G. Bocelli, Y.A. Simonov, A.P. Gulya, *Russ. J. Gen. Chem.* 79 (2009) 428–434.
- [28] K. Alomar, A. Landreau, M. Kempf, M.A. Khan, M. Allain, G. Bouet, *J. Inorg. Biochem.* 104 (2010) 397–404.
- [29] L. Palatinus, G. Chapuis, *J. Appl. Crystallogr.* 40 (2007) 786–790.
- [30] V. Petricek, M. Dusek, L. Palatinus, *Z. Kristallogr* 229 (2014) 345–352.
- [31] Diamond – Crystal and Molecular Structure Visualization. Crystal Impact – K. Brandenburg & H. Putz GbR, Rathaugasse 30, D-53111 Bonn.
- [32] E. Vinuelas-Zahinos, F. Luna-Giles, P. Torres-Garcia, M.C. Fernandez-Calderon, *Eur. J. Med. Chem.* 46 (2011) 150–159.
- [33] M. Khandani, T. Sedaghat, N. Erfani, M.R. Haghshenas, H.R. Khavasi, *J. Mol. Struct.* 1037 (2013) 136–143.